Nanoscale Magnesium Hydroxide and Magnesium Oxide Powders: Control over Size, Shape, and Structure via Hydrothermal Synthesis

Yi Ding,[†] Guangtao Zhang,[†] Hao Wu,[†] Bin Hai,[†] Liangbin Wang,[‡] and Yitai Qian*[,†,‡]

Department of Chemistry, and Structure Research Laboratory, University of Science and Technology of China, Hefei 230026, People's Republic of China

Received July 25, 2000. Revised Manuscript Received November 1, 2000

$Mg(OH)_2$ nanocrystallines with rod-, tube-, needle-, or lamella-like morphologies have been synthesized by a hydrothermal reaction using different magnesium precursors and solvents as the reactants. The products appeared to have narrow size distributions with a monodisperse nature. Subsequent thermal decomposition at 450 °C gave nanosized MgO, which preserved well the morphological features of the $Mg(OH)_2$ samples. The specific surface areas of the MgO samples were determined by the BET technique, which gave a feature of high surface area generally larger than 100 m^2/g. The channels formed in the thermal dehydroxylation process may account for this feature of the MgO nanocrystallines.

1. Introduction

Magnesium oxide (MgO, periclase), as an exceptionally important material for use in catalysis,[1,2] toxic waste remediation[3], or as additives in refractory, paint, and superconductor products,[4−6] has been attracting both fundamental and application studies.[6−10] The most conventional method for synthesis of MgO is the decomposition of various magnesium salts or magnesium hydroxide ($Mg(OH)_2$, brucite).[4,11−13] However, the MgO products based on this method usually exhibit relatively large and varied grain sizes, inhomogeneous morphologies, and small surface areas, all of which are disadvantageous for their use in the application field. Therefore, a new and inexpensive method to produce nanosized MgO with narrow size distribution, controllable structure and morphology, and larger specific surface area is necessary. One method to prepare nanosized MgO is the sol−gel technique.[14,15] Klabunde et al.[16,17] once prepared ultrahigh surface area $Mg(OH)_2$ and MgO powders with sizes of about 5 nm via a sol−gel technique followed by a hypercritical drying procedure. However, the need to synthesize and handle the costly and hazardous metal-organic precursors in the sol−gel procedure seems inconvenient and also not economically acceptable. Recently, we successfully synthesized rod-like and tube-like $Mg(OH)_2$ nanocrystallines through a very simple hydrothermal technique.[18] Further investigations demonstrated that the crystallite size, shape, and structure of the obtained nanoparticles could be controlled well by this method, even with the most commonly used magnesium salts or magnesium powder.

In this paper, we describe an approach for controlling these characteristics of nanosized $Mg(OH)_2$ through this hydrothermal route. MgO nanocrystallines from the thermal decomposition of thus-prepared $Mg(OH)_2$ products were also investigated and we found the obtained MgO did show a high surface area feature.

2. Experimental Section

The $Mg(OH)_2$ nanocrystalline samples were prepared by the hydrothermal method using different magnesium sources, such as Mg powder, $MgSO_4$, and $Mg(NO_3)_2{\cdot}6H_2O$. All reagents were analytical grade pure and were purchased from Shanghai Chemical Co. Ltd. In a typical procedure, 0.01 mol of powder magnesium sources were added into a Teflon-lined autoclave

---

* To whom correspondence should be addressed.

[†] Department of Chemistry.

[‡] Structure Research Laboratory.

(1) Liang, S. H. C.; Gay, I. D. *J. Catal.* **1986**, *101*, 293.

(2) Tsuji, H.; Yagi, F.; Hattori, H.; Kita, H. *J. Catal.* **1994**, *148*, 759.

(3) Copp, A. N. *Am. Ceram. Soc. Bull.* **1995**, *74*, 135.

(4) Bhargava, A.; Alarco, J. A.; Mackinnon, I. D. R.; Page, D.; Ilyushechkin, A. *Mater. Lett.* **1998**, *34*, 133.

(5) Yuan, Y. S.; Wong, M. S.; Wang, S. S. *J. Mater. Res.* **1996**, *11*, 8.

(6) Yang, P. D.; Lieber, C. M. *Science* **1996**, *273*, 1836.

(7) Wagner, G. W.; Bartram, P. W.; Koper, O.; Klabunde K. J. *J. Phys. Chem. B* **1999**, *103*, 3225.

(8) Boldyrev, A. I.; Simons, J. *J. Phys. Chem.* **1996**, *100*, 8023.

(9) Ye, X. S.; Sha, J.; Jiao, Z. K.; Zhang, L. D. *Nanostruct. Mater.* **1997**, *8*, 945.

(10) Sterrer, M.; Diwald, O.; Knozinger, E. *J. Phys. Chem. B* **2000**, *104*, 3601.

(11) Ardizzone, S.; Bianchi, C. L.; Vercelli, B. *Appl. Surf. Sci.* **1998**, *126*, 169.

(12) Ardizzone, S.; Bianchi, C. L.; Vercelli, B. *J. Mater. Res.* **1998**, *13*, 2218.

(13) Beruto, D.; Botter, R.; Searcy, A. W. *J. Am. Ceram. Soc* **1987**, *70*, 155.

(14) Wang, J. A.; Novaro, O.; Bokhimi, X.; Lopez, T.; Gomez, R.; Navarrete, J.; Llanos, M. E.; Lopez-Salinas, E. *J. Phys. Chem. B* **1997**, *101*, 7448.

(15) Wang, J. A.; Novaro, O.; Bokhimi, X.; Lopez, T.; Gomez, R.; Navarrete, J.; Llanos, M. E.; Lopez-Salinas, E. *Mater. Lett.* **1998**, *35*, 317.

(16) Utamapanya, S.; Klabunde, K. J.; Schlup, J. R. *Chem. Mater.* **1991**, *3*, 175.

(17) Koper, O. B.; Lagadic, I.; Volodin, A.; Klabunde, K. J. *Chem. Mater.* **1997**, *9*, 2468.

(18) Li, Y. D.; Sui, M.; Ding, Y.; Zhang, G.; Zhuang, J.; Wang, C. *Adv. Mater.* **2000**, *12*, 818.

10.1021/cm000607e CCC: $20.00

Table 1. $Mg(OH)_2$ Nanocrystallines Obtained in Different Experimental Conditions (*: in Volume Ratio)

sample no.	magnesium source	solvent	temp (°C)	time (h)	phase	morphology	size (nm, TEM)
1	Mg	en−H_2O (8:1)*	180	20	$Mg(OH)_2$ hexa.	rod-like	20 × 200
2	Mg	en−H_2O (1:6)*	180	20	$Mg(OH)_2$ hexa.	lamellar	50−100
3	Mg	NH_3·H_2O (pH 10)	180	20	$Mg(OH)_2$ hexa.	lamellar, tube-like	25−200, 40 × 600
4	$MgSO_4$	en−H_2O (4:1)*	180	20	$Mg(OH)_2$ hexa.	needle-like	10−20 × 50−100
5	$MgSO_4$	en−H_2O (1:1)*	180	20	$Mg(OH)_2$ hexa.	lamellar	100−150
6	$MgSO_4$	NH_3·H_2O (pH 11)	110	20	$Mg(OH)_2$ hexa.	lamellar	150
7	$Mg(NO_3)_2$·$6H_2O$	en	180	20	$Mg(OH)_2$ hexa.	lamellar	80−100
8	$Mg(NO_3)_2$·$6H_2O$	NH_3·H_2O (pH 10)	180	20	$Mg(OH)_2$ hexa.	lamellar	100−200
9	$Mg(NO_3)_2$·$6H_2O$	NaOH (0.1 M)	80	2	$Mg(OH)_2$ hexa.	lamellar	50

of 60-mL capacity, respectively. Then, the autoclave was filled with various solvents (ethylenediamine solution, aqueous ammonia, or dilute NaOH solution) up to 70% of the total volume and kept at the set reaction temperature (for example, 180 °C) for 2−20 h. After cooling to room temperature naturally, the white $Mg(OH)_2$ powders were collected, washed with distilled water and absolute ethanol several times, and then dried in a vacuum at 60 °C for 4 h.

Some of the obtained $Mg(OH)_2$ samples were subsequently calcined in air in a muffle furnace using a step temperature controller. The samples were first held at 280 °C for 1 h, then at 350 °C for 2 h, and finally at 450 °C for 2 h. The temperature was increased very slowly to maximally avoid the sudden collapse of the brucite structure, so as to preserve the morphological features of the $Mg(OH)_2$ nanocrystallines in the final MgO products.

Phase identification was done by the X-ray diffraction (XRD) technique, using Cu Kα (λ = 1.54056 Å) radiation on an MXP18AHF X-ray diffractometer (MAC Science Co. Ltd.). Morphology and structure investigations were performed with a Hitachi (H-800) transmission election microscope (TEM). Thermal behavior of the $Mg(OH)_2$ powders were studied through thermogravimetric analysis (TGA) and differential thermal analysis (DTA), which were collected with a Shimadzu-50 thermoanalyzer apparatus under N_2 flow. The specific surface areas of the finally obtained MgO nanocrystallines were determined from the nitrogen absorption data at liquid nitrogen temperature using the Brunauer−Ennett−Teller (BET) technique by means of a Micromeritics ASAP 2000 apparatus.

3. Results and Discussion

3.1. $Mg(OH)_2$ Section. As will be seen below, the $Mg(OH)_2$ nanocrystallines from this hydrothermal route have some very interesting characteristics. Even a slight change of the reaction condition will strongly affect the structural and morphological features of the resulting $Mg(OH)_2$ particles. The results under different conditions are summarized in Table 1.

A typical XRD pattern is given in Figure 1a (for sample 9). All diffraction peaks in Figure 1a can be indexed as the hexagonal structure magnesium hydroxide (JCPDS file number 7-239). The significant peak broadening indicates the $Mg(OH)_2$ has a very small grain size. It is noted that the crystallite size, estimated by means of the Debye−Scherrer formula[19] based on the full width at half-maximum (fwhm) of different diffraction peaks, has different values (Table 2), for example, 6.86 nm (001), 9.66 nm (101), and 18.8 nm (110), which indicates that the particles have a morphology of thin plate shape with layers in the [001] direction. This is supported by the TEM studies shown below, which demonstrate sample 9 does exhibit a hexagonal lamella-like structure.

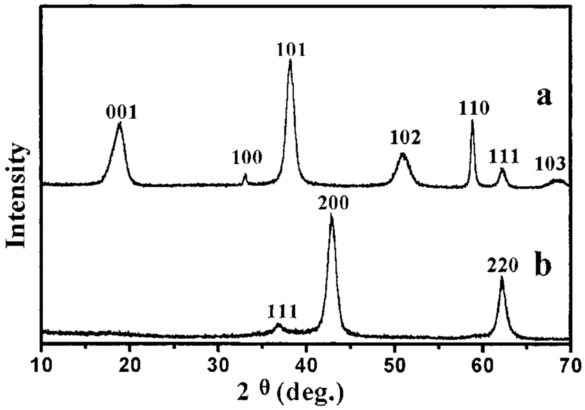

Figure 1. X-ray diffraction (XRD) patterns of $Mg(OH)_2$ (a) and MgO (b) powders for sample 9.

Table 2. Crystal Data and Crystallite Size Information from the XRD Patterns of $Mg(OH)_2$ and MgO (for Sample 9)

	peak position (*d* value, Å)	Miller indices (*hkl*)	fwhm (deg)	crystallite size (nm) (estimated by Scher. equation)
$Mg(OH)_2$ hexa.	4.765	001	1.16	6.86
	2.362	101	0.86	9.66
	1.791	102	1.24	7.02
	1.568	110	0.48	18.8
	1.492	111	0.70	13.1
MgO cubic	2.112	200	0.88	9.6
	1.492	220	0.68	13.5

3.1.1. Magnesium Route. Transmission electron microscope (TEM), a powerful method for structure analysis at a nanometer scale, allows for direct observation of the morphological and structural features of the $Mg(OH)_2$ samples.

First, a forced hydrolysis process of metal magnesium powder is investigated. Reactions of powder Mg with mixed solvents of ethylenediamine (en) and water in

---

[19] Klug, H. P.; Alexander, L. E. *X-ray Diffraction Procedures*; Wiley: New York, 1962.

different volume ratios give different results. When a mixture of en and H_2O in a volume ratio of 8:1 is tried, the $Mg(OH)_2$ products exhibit rod-like morphology[18] with a diameter of about 20 nm and length typically exceeding 200 nm (Figure 2a, sample 1). When H_2O is used in excess, (e.g., en:H_2O = 1:6), the products display a hexagonal lamellar morphology with a size of 50−100 nm (Figure 2b, sample 2). Some $Mg(OH)_2$ particles are found standing straight on the copper grid, which demonstrates that these lamellae have a thickness of about 10 nm. These results are actually expected because the chelating agents such as ethylenediamine were found to have an exceptional effect in preparing one-dimensional materials.[20] Although the true mechanism of the effect is still unclear, the selective interaction between the coordinating solvents and surface ions is thought to have the ability to slow the growth of specific lattice planes and thus cause the expression of these crystal planes in the final crystal form.[21] When aqueous ammonia is used as the solvent (sample 3), the $Mg(OH)_2$ products mainly display a lamellar shape with an inhomogeneous size distribution from 25 to 200 nm. However, this drawback (of inhomogeneity) can be fully counteracted by the coexistence of a fascinating structure—tubular $Mg(OH)_2$ nanocrystalline. Figure 2c shows such a nanotube structure, with 8-nm inner diameter, 40-nm outer diameter, and length of no less than 600 nm. An electron diffraction pattern (Figure 2d) recorded on this nanotube reveals a hexagonal tube structure with a preferential direction for nanotube growth. The ED pattern recorded on lamellar particles is also shown for comparison (Figure 2e), which exhibits a typical hexagonal diffraction feature along the [001] zone axis direction. It is admitted that the preparation of the tubular structure is not so novel today, especially for materials with a layered structure.[22,23] The appearance of a nanotube structure in such a simple reaction is still exciting. From the TEM observation, the nanotube $Mg(OH)_2$ only shows a very minute quantity in the whole sample, but this reaction is very reproducible and these nanotubes can always be found. Recent investigation has shown that large amounts of nanotube $Mg(OH)_2$ could be obtained by electrolyzing the sheet magnesium under proper reaction conditions.[24]

3.1.2. Magnesium Sulfate Route. Samples 4−6 are prepared using magnesium sulfate ($MgSO_4$) as the reactant. When mixed solvent en−H_2O (4:1) is used, needle-shaped $Mg(OH)_2$ can be obtained. Figure 2f exhibits these slightly aggregated particles, having a small size of 10−20 nm in diameter and 50−100 nm in length. The corresponding ED pattern (Figure 2g) shows two diffuse diffraction rings, indicative of a fine crystallite size character. Further increasing the volume ratio of en to H_2O will result in a coordination compound instead of $Mg(OH)_2$, consisting of Mg^{2+}, SO_4^{2-}, and en, while increasing the relative amount of water to en:H_2O 1:1 will result in a 100−150-nm polygonal thin plate (Figure 2h, sample 5). Reaction of $MgSO_4$ with $NH_3\cdot H_2O$ at 110 °C can produce a beautiful, hexagonal plate-shaped $Mg(OH)_2$ with a uniform size of 150 nm (sample 6). Reaction temperature above 110 °C will result in superstructured $Mg(OH)_2-MgSO_4-H_2O$ whiskers.[25]

3.1.3. Magnesium Nitrate Route. When $Mg(NO_3)_2\cdot 6H_2O$ is used as the magnesium source, the obtained $Mg(OH)_2$ nanocrystallines always show hexagonal lamella shape, no matter whether en or aqueous ammonia is used. It should be pointed out that reaction of $Mg(NO_3)_2\cdot 6H_2O$ with *pure* en can produce *pure* uniform-sized $Mg(OH)_2$ nanocrystallines in a high yield (80−100 nm, Figure 2i, sample 7). The hydration water in $Mg(NO_3)_2\cdot 6H_2O$ seems enough to ensure a completion of this reaction. This is quite different from that of the $MgSO_4$ case. Why will a simple anion change from SO_4^{2-} to NO_3^- cause such a dramatic change in this hydrolysis reaction? A possible explanation is that magnesium nitrate cannot react with ethylenediamine to form a stable coordination compound, for example, the $Mg(en)_x(NO_3)_2\cdot yH_2O$ phase, or if a similar coordination compound does exist, it must show large solubility in both en and water so as to diminish the effect of en in competition with OH^- for Mg^{2+}.

It is also beyond our expectations that direct mixing of the dilute solutions of $Mg(NO_3)_2\cdot 6H_2O$ and NaOH, followed by a subsequent hydrothermal aging process at 80 °C for 2 h, can produce nearly monodispersed $Mg(OH)_2$ nanoparticles with an average size of 50 nm (Figure 2j, sample 9). Dilute solutions of $Mg(NO_3)_2\cdot 6H_2O$ and NaOH with concentrations less than 0.1 M as well as a subsequent aging process are needed to avoid the rapid formation of severely aggregated $Mg(OH)_2$ nanoparticles with poor crystallinity. Electron diffraction pattern (Figure 2k) also confirms the hexagonal structure, and diffraction rings of planes 002, 101, 110, and so on can be clearly seen.

3.1.4. TGA and DTA Analyses. The TGA−DTA technique was used to analyze the thermal behavior of the $Mg(OH)_2$ samples and thus could provide the necessary data for the following decomposition process. A typical TGA−DTA profile is shown in Figure 3, which corresponds to sample 3. One can see from this profile only a pronounced weight loss step is found in the temperature range of 280−450 °C and a corresponding endothermic peak is observed near 352 °C. This can be ascribed to the decomposition of brucite:

$$Mg(OH)_2 \xrightarrow{-H_2O} MgO$$

However, in terms of the above reaction, about 30.8% weight loss should be achieved, which is slightly larger than the observed 27.7%. We owe it to the incompleteness of the decomposition reaction in this temperature range. This is consistent with the previous reports.[15,26]

3.2. MgO Section. Samples 2, 4, 5, 7, and 9 have shown homogeneous morphologies with narrow size distributions and thus were chosen to undergo a subsequent calcination process to obtain MgO nanocrystallines. Figure 1b displays an XRD pattern of cubic

---

(20) Li, Y. D.; Liao, H. W.; Ding, Y.; Qian, Y. T.; Yang, L.; Zhou, G. E. *Chem. Mater.* **1998**, *10*, 2301.

(21) Doxsee, K. M.; Chang, R. C.; Chen, E.; Myerson, A. S.; Huang, D. P. *J. Am. Chem. Soc.* **1998**, *120*, 585.

(22) Hacohen, Y. R.; Grunbaum, E.; Tenne, R.; Sloan, J.; Hutchison, J. L. *Nature* **1998**, *395*, 336.

(23) Tenne, R.; Margulis, L.; Genut, M.; Hodes, G. *Nature* **1992**, *360*, 444.

(24) Mo, X.; Chen, Z. Y., unpublished results.

(25) Ding, Y.; Zhang, G. T.; Zhang, S. Y.; Huang, X. M.; Yu, W. C.; Qian, Y. T. *Chem. Mater.* **2000**, *12*, 2845.

(26) Ardizzone, S.; Bianchi, C. L.; Fadoni, M.; Vercelli, B. *Appl. Surf. Sci.* **1997**, *119*, 253.

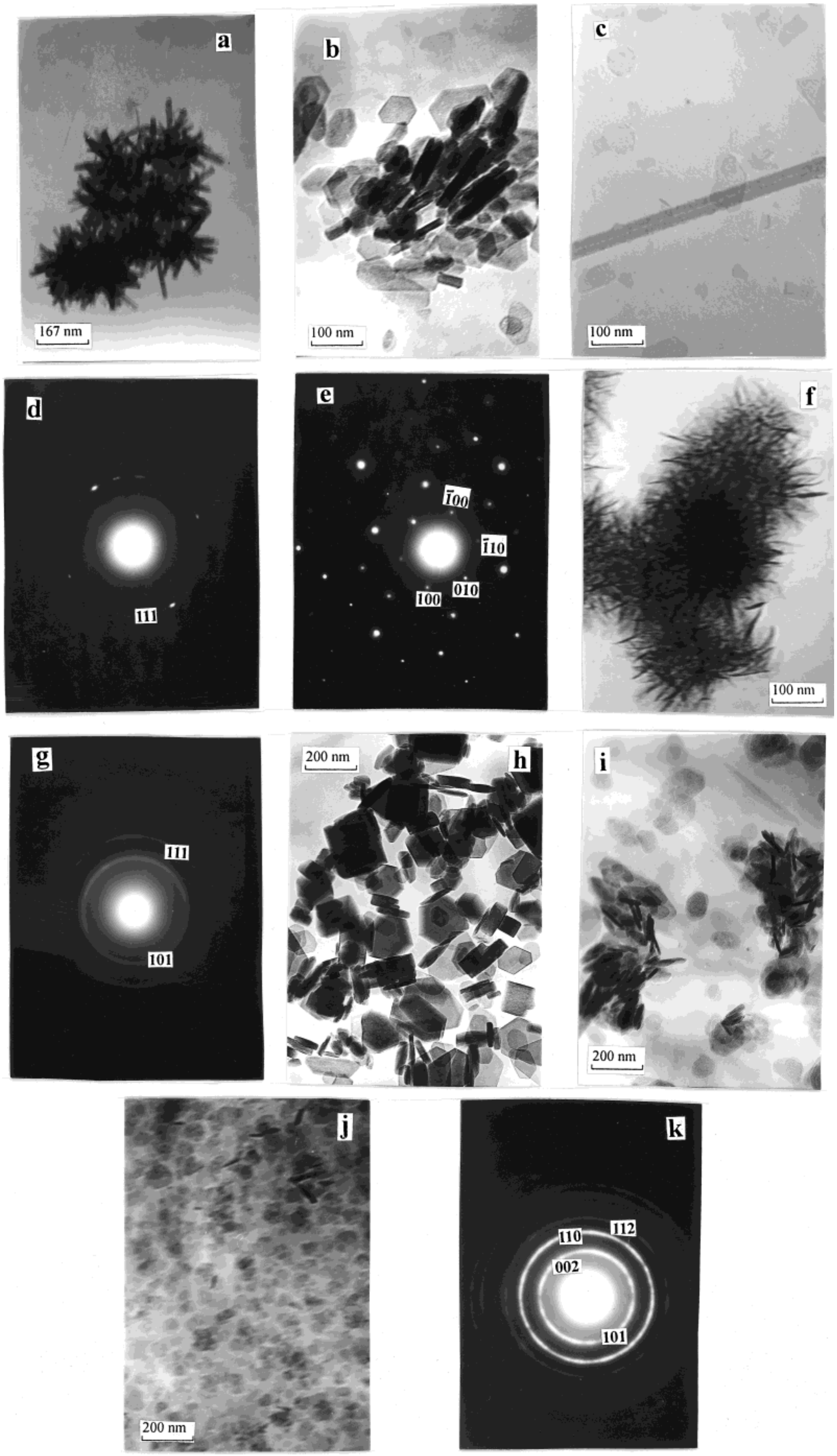

Figure 2. TEM images and diffraction patterns of the $Mg(OH)_2$ nanocrystallines: (a) sample 1, Mg in ethylenediamine (en:H_2O = 8.:1); (b) sample 2, Mg in ethylenediamine (en:H_2O = 1:6); (c)–(e) sample 3, Mg in NH_3·H_2O; (f),(g) sample 4, $MgSO_4$ in ethylenediamine (en:H_2O = 4:1); (h) sample 5, $MgSO_4$ in ethylenediamine (en:H_2O = 1:1); (i) sample 7, $Mg(NO_3)_2$·$6H_2O$ in ethylenediamine; (j),(k) sample 9, $Mg(NO_3)_2$·$6H_2O$ in NaOH (0.1 M).

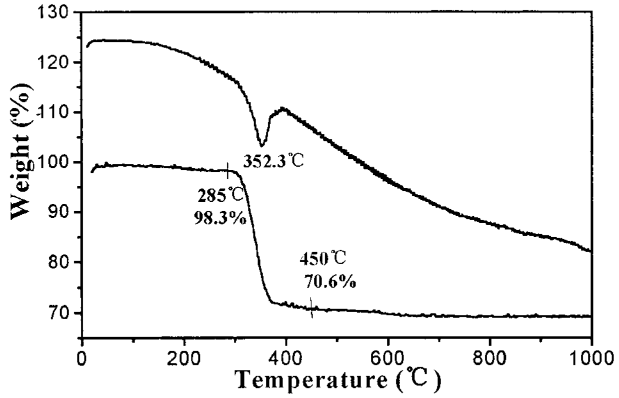

Figure 3. TGA−DTA trace of sample 3 heated in N_2 flow from 20 to 1000 °C.

structure MgO (from sample 9). It is interesting to note that the estimated crystallite sizes are 9.6 nm for the (200) plane and 13.5 nm for the (220) plane, which are nearly the same with the values from the (101) and (111) reflections of its magnesium hydroxide precursor (Table 2). It is admitted that direct comparison of the crystallite sizes from Scherrer estimation is less meaningful, provided that the particle dimension is not the only reason to account for the peak broadening; especially here the lattice distortion of MgO nanocrystallines is obviously significant. However, this fact still supposes that a morphological preservation might be achieved during the structure rearrangement process of a hexagonal structure ABAB... into a cubic structure ABCABC.... This is supported by the TEM images shown in Figure 4. From Figure 4a, the needle-shape feature of $Mg(OH)_2$ (sample 4) is fully retained in the final MgO samples.

Table 3 reports the specific surface areas (*S*) for the above five MgO samples. Particle sizes based on TEM and XRD studies are also included for comparison. It is found that the values of the specific surface areas of the MgO samples from this hydrothermal method are generally larger than 100 m^2/g, much larger than the reported data for the salt-decomposition MgO,[11,12,27] and fully comparable with the values for the sol−gel MgO.[16,17] The MgO nanocrystallines from sample 5 have the smallest crystallite size (7.9 nm, XRD) and thus have the largest BET value of 161.49 m^2/g. In contrast, sample 2 shows the lowest surface area because it has a relatively larger crystallite size (11.1 nm).

It is noted that the particle sizes from TEM observations are systematically larger than corresponding XRD values. This means that the observed lamella-like MgO particles are actually composed of much smaller crystallites. It is known that during the thermal dehydroxylation process water molecules are formed and lost between the two adjacent layers of hydroxyl ions, leaving a periclase structure with many defects and irregular intercrystallite channels (cracks). These channels may be the main cause of the high surface area-to-volume ratio feature of the MgO nanocrystallines. And these channels can also be clearly seen in Figure 4b (sample 7).

From the BET values, the particle size can be estimated according to the formula $d_p = 6 \times 10^3/S\rho$, where d_p is the size of particles (nm), *S* is the specific surface area (m^2/g), and ρ is the density of MgO (3.58 g/cm^3).[28] This formula assumes that the particles have a cubic (or spherical) configuration with uniform size distribution and low surface roughness. The particle sizes thus-estimated are also listed in Table 3, which are slightly larger than the crystallite sizes by XRD analysis.

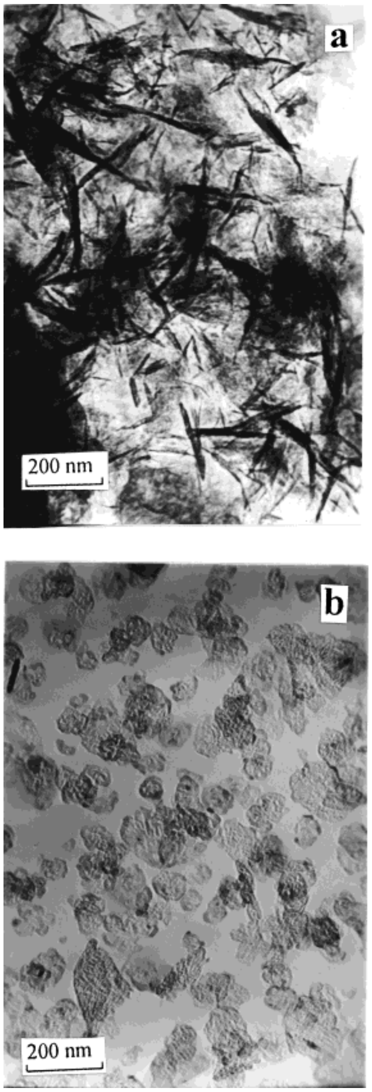

Figure 4. TEM images of the MgO nanocrystallines (a) from sample 4 and (b) from sample 7.

Table 3. Specific Surface Area Values and the Estimated Particle Sizes of MgO Samples (* Based on (200) Plane)

sample no.	*S* (m^2/g)	particle size (nm, BET)	crystallite size* (nm, XRD)	particle size (nm, TEM)	morphology
2	122.05	13.73	11.1	50−100	lamellar
4	132.21	12.68	10.0	20−40 × 100−200	needle-like
5	161.49	10.38	7.9	100−150	lamellar
7	147.71	11.35	8.7	50−100	lamellar
9	143.37	11.69	9.6	20−40	lamellar

4. Conclusion

A hydrothermal reaction has been employed to synthesize nanosized $Mg(OH)_2$. The results show that the

---

[27] Choundhary, V. R.; Rane, V. H.; Gadre, R. V. *J. Catal.* **1994**, *145*, 300.

[28] Weast, R. C. *CRC Handbook of Chemistry and Physics, 66th edition*; CRC Press: Boca Raton, FL, 1986.

characteristics of the products, such as the crystallite size, shape, and structure, can be controlled well by choosing different solvents and reaction conditions. Nanosized MgO products are produced by a subsequent thermal decomposition of their $Mg(OH)_2$ precursors. And the morphological features of the starting products are retained well during this thermal transformation process. These MgO nanocrystallines exhibit a high specific surface area feature, which might suggest their potential value for use in the catalysis field.

Acknowledgment. We thank Prof. S. Y. Zhang, Dr. L. Chen, X. M. Huang, L. Yang, and J. Lu for helpful discussions and assistance with the XRD and TEM studies. This work is supported by the National Natural Science Foundation of China and the National Nanometer Materials Climbing Project.

CM000607E